

Sunil S. Damodhar* and S. Krishna

A Novel Load Shedding Scheme for Voltage Stability

DOI 10.1515/ijeeps-2015-0159

Abstract: Undervoltage load shedding serves to maintain voltage stability when a majority of loads are fast acting. An undervoltage load shedding scheme should address two tasks: the detection of voltage instability following a large disturbance and the determination of the amount of load to be shed. Additionally, in case of short-term voltage instability, the scheme should be fast. This paper proposes a method to predict voltage instability arising due to a large disturbance. The amount of load to be shed to maintain voltage stability is then determined from the Thevenin equivalent of the network as seen from the local bus. The proposed method uses local measurements of bus voltage and power, and does not require knowledge of the network. The method is validated by simulation of three test systems subjected to a large disturbance. The proposed scheme is fairly accurate in estimating the minimum amount of load to be shed to maintain stability. The method is also successful in maintaining stability in cases where voltage collapse is detected at multiple buses.

Keywords: load shedding, voltage stability, dynamic load

1 Introduction

Undervoltage load shedding is a viable solution to the voltage stability problem in power systems. Load shedding may be employed as a last resort and can be justified, as in its absence, the abnormal voltage leads to tripping of loads. The load buses where voltage collapse can occur, need to be identified. Once these buses are identified, the amount of load to be shed needs to be determined. Ideally, the amount of load shed should be minimal, just enough to prevent instability. For avoiding short-term voltage instability, load shedding has to be carried out as fast as possible. This calls for a fast method

for predicting instability and providing an estimate of the minimum amount of load to be shed to maintain stability.

Several schemes for load shedding to prevent voltage instability have been suggested in literature. The need for load shedding to maintain voltage stability, especially when there is large penetration of motor loads, is discussed in Taylor [1]. The paper suggests fixing the amount of load to be shed beforehand. Load shedding is proposed to be carried out with reference to the drop in voltage observed at specific delays. The load shedding scheme based on static load models presented in Tuan et al. [2] proposes indicators at the buses and relates their sensitivity to the amount of load to be shed. The method, however, ignores the dynamic aspects of voltage instability. Short term voltage instability is a fast phenomenon and load dynamics cannot be ignored.

An iterative load-shedding scheme for long-term voltage stability, with loads represented by dynamic models is presented in Arnborg et al. [3]. A scheme based on tracking Thevenin equivalent for sensing instability is presented in Vu et al. [4]. An undervoltage load shedding scheme using the generic dynamic load model Xu and Mansour [5] is presented in Balanathan et al. [6]. The method measures bus voltage and power to determine the amount of load to be shed and discusses an online method for estimating the parameters of the load. In Balanathan et al. [7], a proximity indicator based on the Thevenin equivalent is used to determine the amount of load to be shed. The proximity indicator presented in Vu et al. [4] is used to decide the location and timing of load shedding. An improvement of the proximity indicator is suggested in Wiszniewski [8]. The methods based on proximity indicators, which wait for the operating point to traverse the nose point of the PV curve, may not be suitable while addressing a fast phenomenon. Further, delayed action would mean larger amount of load to be shed to maintain stability. It is therefore necessary to predict instability before the nose point is reached.

In this work, undervoltage load shedding, when bulk of loads are fast-acting, is addressed. Voltage instability, immediately following a large disturbance, is predicted. A load shedding scheme that determines the amount of load that has to be shed in order to prevent voltage instability is developed. The method requires only local

*Corresponding author: Sunil S. Damodhar, Department of Electrical Engineering, Indian Institute of Technology Madras, ESB 340, Chennai, Tamil Nadu 600036, India, E-mail: ee09d006@ee.iitm.ac.in
S. Krishna, Department of Electrical Engineering, Indian Institute of Technology Madras, Chennai, Tamil Nadu 600036, India, E-mail: krishnas@ee.iitm.ac.in

measurements of bus voltage magnitude and bus active, reactive powers. The scheme is validated using simulations. Results for the 9-bus, 39-bus and 162-bus systems are presented. The method is found to be successful in detecting instability and in maintaining the stability of the system through load shedding at buses where instability is detected. In cases where voltage instability is detected only at a single bus, the method accurately determines the minimum amount of load to be shed to maintain stability. The method is also successful in maintaining stability when voltage collapse is observed at multiple buses.

The main contributions of the paper are:

1. A method is proposed to predict voltage instability arising due to a large disturbance. The method relies only on local measurements.
2. The paper proposes a method of determining the amount of load to be shed in order to avoid voltage instability.
3. The proposed method is validated by simulation studies on three test systems.

2 Single load connected to infinite bus

The most predominant loads are induction motor loads which tend to consume constant power following a change in voltage. Henriques et al. [9] shows how adequate modeling of induction motor loads helps in better prediction of system behaviour. The first-order dynamic model Abe et al. [10] serves as a suitable load model. The model has been extensively discussed in literature Sekine and Ohtsuki [11], Ohtsuki et al. [12], Pal [13, 14] The load is described by the differential equation

$$T_L \frac{dG_m}{dt} = P_{L0} - V_m^2 G_m \quad (1)$$

Where T_L , Time-constant of the load; G_m , Conductance of the load; P_{L0} , Initial steady-state active power consumed by the load; V_m , Load internal voltage.

A suitable time-constant may be chosen depending on the load composition IEEE [15]. The equivalent circuit of the load is shown in Figure 1. $V \angle \theta$ and $V_m \angle \theta_m$ are load bus voltage and load internal voltage respectively and X_m denotes the reactance of the load. Equation (1) can be derived from the following basic equation representing motor dynamics.

$$\frac{2H}{\omega_0} \frac{d\omega}{dt} = T_{elec} - T_{mech} \quad (2)$$

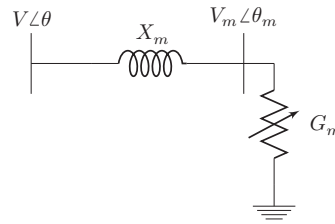


Figure 1: Equivalent circuit of load.

where H is the inertia constant, ω_0 is the synchronous speed, T_{elec} is the electrical torque and T_{mech} is the load torque. The slip s is given by $s = (\omega_0 - \omega) / \omega_0$ and $T_{elec} = V_m^2 (s/r)$, where r is the rotor resistance at standstill. A comparison of eqs (1) and (2) gives $T_L = 2Hr$ and $G_m = s/r$.

The load internal voltage V_m can be expressed in terms of the bus voltage V by the following equation

$$V_m = \frac{V}{\sqrt{1 + G_m^2 X_m^2}} \quad (3)$$

The active and reactive powers drawn by the load are functions of bus voltage V and the load parameters. These are given by

$$\begin{aligned} P_L &= \frac{V^2 G_m}{1 + G_m^2 X_m^2} \\ Q_L &= \frac{V^2 G_m^2 X_m}{1 + G_m^2 X_m^2} \end{aligned} \quad (4)$$

Immediately following a large disturbance, the load first changes according to its instantaneous characteristic (constant impedance) before adjusting the state-variable G_m to meet the demand. The initial values for G_m and X_m can be determined from load flow analysis.

Consider the simple system consisting of a load connected to an infinite bus through a double-circuit lossless transmission line. The infinite bus voltage is V_s . Let the system be operating at the stable equilibrium point. Then, a large disturbance in the form of loss of a transmission line circuit is assumed to occur. The pre-disturbance and the post-disturbance PV curves are shown in Figure 2. Point A is the pre-disturbance stable equilibrium point. Immediately following the disturbance, the operating point jumps to point B on the post-disturbance PV curve and moves towards the stable equilibrium point C. Along the curve AB, the load conductance G_m is equal to the pre-disturbance steady-state value. If the post-disturbance maximum power is greater than P_{L0} , the stable equilibrium point exists and the system is stable. If the post-disturbance maximum power is less than P_{L0} , as shown in Figure 3, the operating point moves along the PV curve

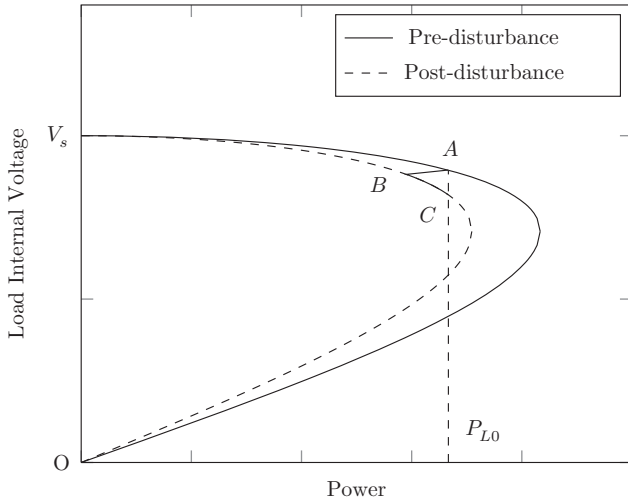


Figure 2: Load connected to infinite bus system, system is stable after a large disturbance.

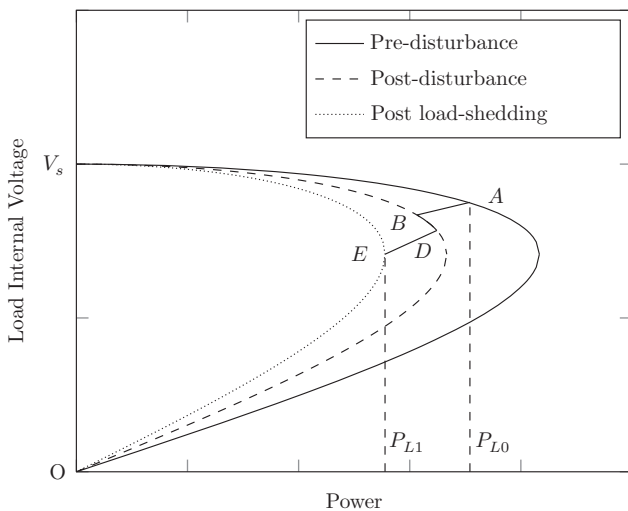


Figure 3: Load shedding for load connected to infinite bus system.

towards the point O , resulting in voltage instability. The system can be stabilized by load-shedding.

Let P_{L1} be the steady-state active power after load-shedding. In order to shed the minimum amount of load and also ensure stability, the post load-shedding equilibrium point should lie on the nose-point of the PV curve. In other words, the post load-shedding maximum power should be equal to P_{L1} . Suppose the load is shed when the system is operating at the point D . Then, the operating point jumps to the nose point E on the post load-shedding PV curve. The curve DE corresponds to a specific value of load conductance G_m . Let X_t be the reactance of a transmission line circuit. Let n denote the ratio of P_{L1} to P_{L0} . Due to load shedding, the

load reactance changes from X_m to X_m/n . For a lossless transmission line,

$$P_{L1} = \frac{V_s^2}{2(X_t + \frac{X_m}{n})} \tag{5}$$

$$\frac{1}{G_{m1}} = X_t + \frac{X_m}{n} \tag{6}$$

where G_{m1} is the steady-state value of the load conductance after load-shedding. From eq. (5),

$$n = \frac{1}{X_t} \left(\frac{V_s^2}{2P_{L0}} - X_m \right) \tag{7}$$

With resistance of the transmission line accounted for, n is obtained by solving the following two equations:

$$n = \frac{V_s^2 \left(\frac{1}{G_{m1}} \right)}{P_{L0} \left[\left(R_t + \frac{1}{G_{m1}} \right)^2 + \left(X_t + \frac{X_m}{n} \right)^2 \right]} \tag{8}$$

$$\frac{1}{G_{m1}} = \sqrt{R_t^2 + \left(X_t + \frac{X_m}{n} \right)^2} \tag{9}$$

where R_t is the resistance of a transmission line circuit. The amount of load to be shed is $(1 - n)P_{L0}$.

3 Detection of instability in a large system

In a large system with multiple loads, voltage instability may be observed at more than one bus. Immediately following a large disturbance, it is necessary to determine whether the load power would recover to the pre-disturbance power. Whenever there is a disturbance such as a loss of a transmission line in a heavily loaded network, it is likely that the voltages drop at the load buses. This type of disturbance can even lead to voltage instability resulting in voltage collapse at some load buses. In order to detect this, it is necessary to monitor the voltages at the load buses; if there is a reduction in voltage, it is necessary to determine if this will eventually lead to voltage instability. Therefore, if the voltage falls below a threshold (predefined) value, it is presumed that a large disturbance might have occurred. In order to determine if this will lead to voltage instability, a curve is fit to the measurements of power at different instants. The maximum value of power on this curve is determined. Voltage instability is predicted if this maximum value is less than the pre-disturbance value of load power. From case studies, a 4th order polynomial was found to give satisfactory results. This

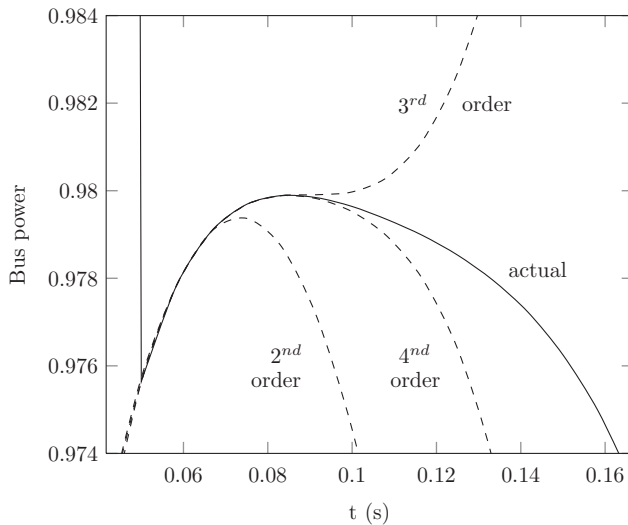


Figure 4: Curves fit at bus 5 of 9-bus system for 2nd, 3rd and 4th polynomial orders.

is illustrated in Figure 4. Curves obtained using the 2nd, 3rd and 4th order polynomials are plotted and compared with the actual curve when a disturbance in the form of loss of a transmission line occurs at $t = 0.05$ s in the 9-bus system. The actual curve of the active power drawn by the load at bus 5 is also shown, the pre-disturbance value of which is 1.25. A comparison of 2nd, 3rd and 4th order polynomials in predicting maximum power, when a large disturbance in the form of loss of a transmission line occurs in each of the 9-bus, 39-bus, and 162-bus systems, is shown in Table 1. P_{\max} is the maximum value of power and t_{\max} is the instant at which P_{\max} occurs. It can be seen that a 4th order polynomial is required for accurate determination of P_{\max} .

4 Load shedding scheme

The strategy for load-shedding given in Section 2 for a single load connected to infinite bus system, can be extended to a large system with multiple loads. The amount of load shed may be deemed to be minimum required if, after shedding, the steady-state operation is at the nose-point of the PV curve. The minimum amount of load to be shed is obtained by determining the Thevenin equivalent of the system as seen from the load bus. If the bus voltage falls by more than 5%, a 4th order polynomial approximation of the bus power as a function of time is obtained to determine the maximum power P_{\max} . If the maximum value predicted by curve fitting is less than the pre-disturbance power, then it can be concluded that voltage instability will occur. When voltage instability is predicted, the Thevenin parameters of the system viz. Thevenin voltage E_{Th} and Thevenin impedance $R_{Th} + jX_{Th}$ are estimated. If there is a disturbance, due to system dynamics, the Thevenin parameters change during the transient. The variation of Thevenin voltage magnitude, Thevenin resistance, and reactance, as seen from bus 35, when a large disturbance in the form of loss of transmission line occurs in the 39-bus system, is shown in Figure 6. It can be seen that the Thevenin parameters only vary slightly in the post-disturbance period.

The magnitude of the load current is

$$I = \frac{E_{Th}}{\sqrt{(R_{Th} + \frac{1}{G_m})^2 + (X_{Th} + X_m)^2}} \quad (10)$$

Values of G_m and X_m can be determined from the load active and reactive powers and the bus voltage. The three unknown quantities E_{Th} , R_{Th} , and X_{Th} can be calculated

Table 1: Comparison of 2nd, 3rd and 4th order polynomials in predicting power maxima.

System	Load bus	Predicted values						Actual values	
		2 nd order		3 rd order		4 th order		P_{\max}	t_{\max}
		P_{\max}	t_{\max}	P_{\max}	t_{\max}	P_{\max}	t_{\max}		
9 bus	5	0.9794	0.0900	0.9799	0.0900	0.9799	0.0849	0.9799	0.0833
39 bus	35	2.7928	0.1035	2.8200	0.1469	2.8199	0.1473	2.8199	0.1499
162 bus	90	0.4325	0.1051	0.4433	0.1946	0.4438	0.1699	0.4432	0.1833
	71	0.2596	0.1022	0.2541	0.1046	0.2609	0.1183	0.2612	0.1334
	85	0.3630	0.1612	0.3631	0.1815	0.3761	0.2018	0.3791	0.2166
	86	0.4776	0.1967	0.4776	0.2047	0.4821	0.2101	0.4884	0.2917
	87	0.1625	0.3055	0.1626	0.4218	0.1637	0.5500	0.1658	0.6000

Table 2: Comparison of Thevenin parameters obtained from (10) with actual values at the end of three measurements.

System	Transmission line tripped	Buses at which voltage collapses	Thevenin parameters					
			Estimated			Actual		
			E_{Th}	R_{Th}	X_{Th}	E_{Th}	R_{Th}	X_{Th}
9-bus	4–5	5	1.113	0.069	0.285	1.097	0.049	0.290
39-bus	35–36	35	0.990	0.002	0.060	0.962	0.006	0.044
162-bus	89–90	90	1.067	0.227	0.479	1.071	0.242	0.460
162-bus	71–150	71	1.054	0.224	0.407	0.983	0.136	0.377
		85	1.048	0.115	0.227	0.966	0.091	0.218
		86	1.035	0.048	0.126	0.960	0.054	0.118
		71	1.055	0.234	0.406	0.984	0.145	0.374
		85	1.050	0.118	0.226	0.964	0.094	0.217
162-bus	149–150	86	1.029	0.047	0.125	0.958	0.054	0.117
		150	0.934	0.201	0.445	0.899	0.180	0.427

using eq. (10) from three sets of measurements at three different instants assuming that they are constant. This method is similar to the methods described in Corsi and Taranto [16], Abdelkader and Morrow [17]. A comparison of the actual Thevenin parameters and the estimated values at the the instant of the third measurement, is shown in Table 2. The Thevenin parameters shown are those seen from buses where instability is predicted as the result of a large disturbance in the form of loss of a transmission line.

The amount of load to be shed is determined using the following equations which are obtained from eqs (8), (9) by replacing V_s , R_t and X_t by E_{Th} , R_{Th} and X_{Th} respectively.

$$n = \frac{E_{Th}^2 \left(\frac{1}{G_{m1}}\right)}{P_{LO} \left[\left(R_{Th} + \frac{1}{G_{m1}}\right)^2 + \left(X_{Th} + \frac{X_m}{n}\right)^2 \right]} \quad (11)$$

$$\frac{1}{G_{m1}} = \sqrt{R_{Th}^2 + \left(X_{Th} + \frac{X_m}{n}\right)^2} \quad (12)$$

For those buses for which n is greater than 1 or less than 0, 100% of the load is shed as it indicates that, after load shedding, there is no equilibrium point. The load-shedding scheme is summarized in Figure 5.

The proposed method is devised for online implementation and involves the following computations:

1. Fitting a 4th order polynomial curve to the power measurements which requires solution of four linear equations, and prediction of P_{max} which requires the solution of a nonlinear equation.

2. Determination of G_m and X_m from the measured values of load active power, load reactive power and bus voltage, using (4).
3. Determination of the Thevenin equivalent parameters E_{Th} , R_{Th} , and X_{Th} by solving three nonlinear equations which are three instances of (10).
4. Determination of the amount of load to be shed by solving the two nonlinear equations (11) and (12).

5 Case studies

The load-shedding scheme is validated through simulation of the 9-bus, 39-bus and 162-bus systems when a large disturbance in the form of loss of a transmission line occurs. The disturbance is assumed to occur at $t = 0.05$ s. Load time-constant $T_L = 0.03$ s. The generators are assumed to be driven by a single reheat steam turbine the data for which are given in Appendix. Simulations are carried out in the programming language [18] Octave.

5.1 9-bus system

The generators of the 9-bus system are represented by the two-axis model. A static exciter having excitation limits $E_{fdmin} = -10$, $E_{fdmax} = +10$ and $K_A = 200$, $T_A = 0.05$ s, is assumed. System data are available in Sauer and Pai [19].

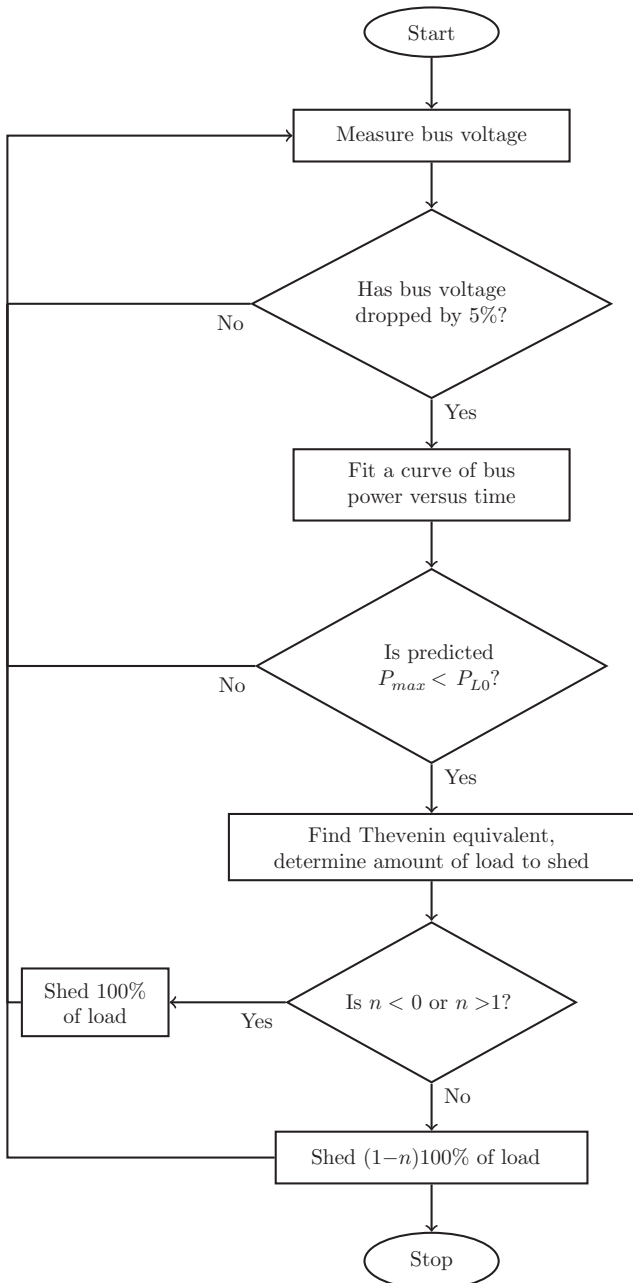


Figure 5: Load shedding scheme.

In the absence of corrective action, the 9-bus system is found to be unstable when the transmission line connecting buses 4 and 5 is tripped. Voltage instability is predicted at bus 5. The proposed scheme makes the system stable by shedding 38.84% of load at bus 5. To maintain stability, the minimum amount of load to be shed at bus 5, obtained by trial and error, is found to be 31%. The bus voltage and internal voltage of bus 5, with and without load-shedding and the trajectory along the PV curves are shown in Figure 7.

5.2 39-bus system

The generators of the 39-bus system are represented by the two-axis model with static exciter. System data are available in Padiyar [20].

The 39-bus system is found to be unstable when the transmission line connecting buses 35 and 36 is tripped. Voltage collapse leading to instability is predicted at bus 35. The proposed scheme makes the system stable by shedding 33.02% of load at bus 35. By trial and error, the minimum amount of load to be shed to maintain stability is found to be 29%. Figure 8 shows the bus voltage and internal voltage of bus and the trajectory along the PV curves of bus 35.

5.3 162-bus system

The generators of the 162-bus system are represented by the classical model. It is assumed that the value of damping coefficient D of the generators is given by $\frac{D\omega_B}{2H} = 0.1$, where ω_B is the base angular frequency and H is inertia constant. System data are available in [21].

The 162-bus system is found to be unstable in three cases: tripping of transmission lines 89–90, 71–150, and 149–150. When the transmission line connecting buses 89 and 90 is tripped, voltage instability is predicted only at bus 90 of the system. Voltage stability is achieved by shedding 20.31% of load at bus 90 using the proposed scheme. The minimum amount of load to be shed at bus 90, to maintain stability, is found to be 20%. The bus voltage and internal voltage of bus 90, with and without load shedding are shown in Figure 9; the trajectory along the PV curves are also shown.

Voltage instability is predicted at multiple buses when either of the transmission lines 71–150 and 149–150 is tripped. When the transmission line 71–150 is tripped, voltage instability is predicted at buses 71, 85 and 86. When the transmission line 149–150 is tripped, voltage instability is predicted at buses 71, 85, 86 and 150. In both the cases, a valid value for $n(0 \leq n \leq 1)$ is obtained only for bus 71. At the other buses, the calculated value of n does not lie between 0 and 1; this means that if load-shedding is done at any of these buses alone, equilibrium point does not exist and the system does not stabilize. At such buses, 100% of the load is shed. The bus voltage and internal voltages of buses where voltage collapses, with and without load-shedding are shown in Figures 10 and 11. The trajectory along the PV curves of bus 71 are also shown. The impact of load-shedding at

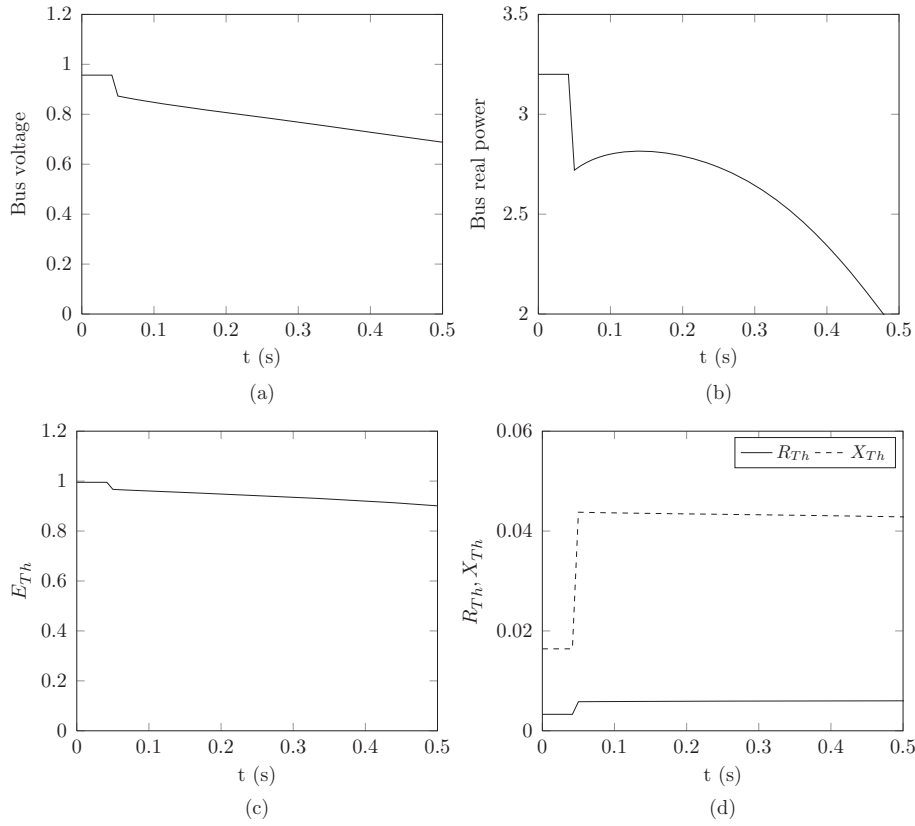


Figure 6: (a) Bus 35 voltage (b) real power (c) and (d) variation of Thevenin parameters of the 39-bus system, as seen from bus 35.

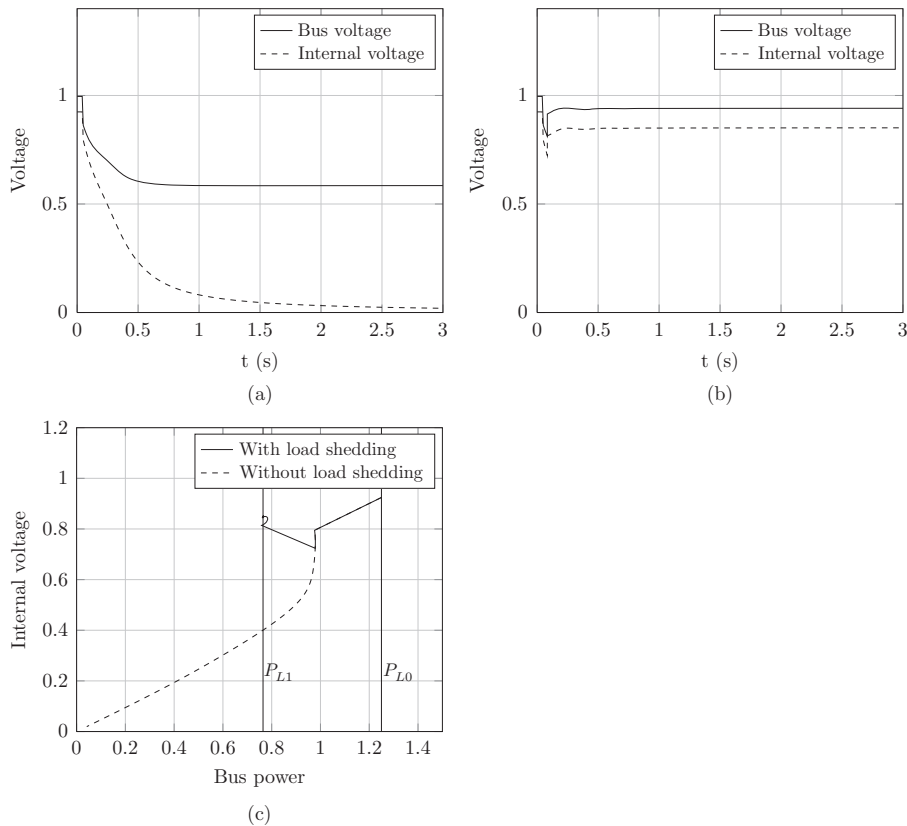


Figure 7: Bus voltage and internal voltage of bus 5 of 9-bus system (a) without load shedding (b) with load shedding, (c) PV curves.

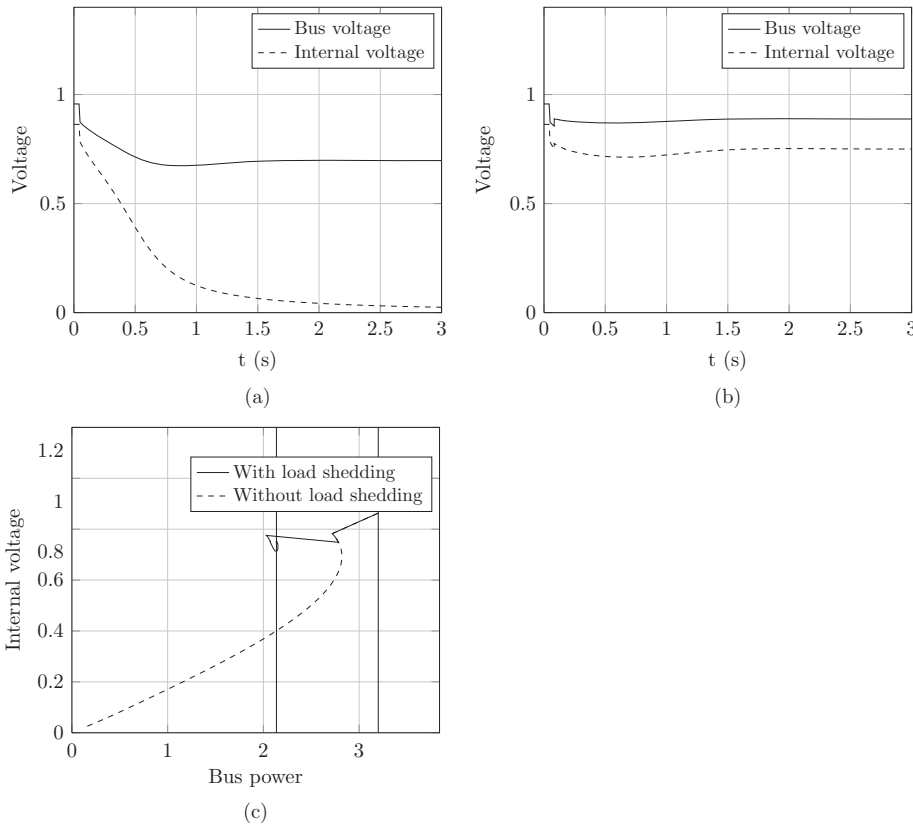


Figure 8: Bus voltage and internal voltage of bus 35 of 39-bus system (a) without load shedding (b) with load shedding, (c) bus 9 PV curves.

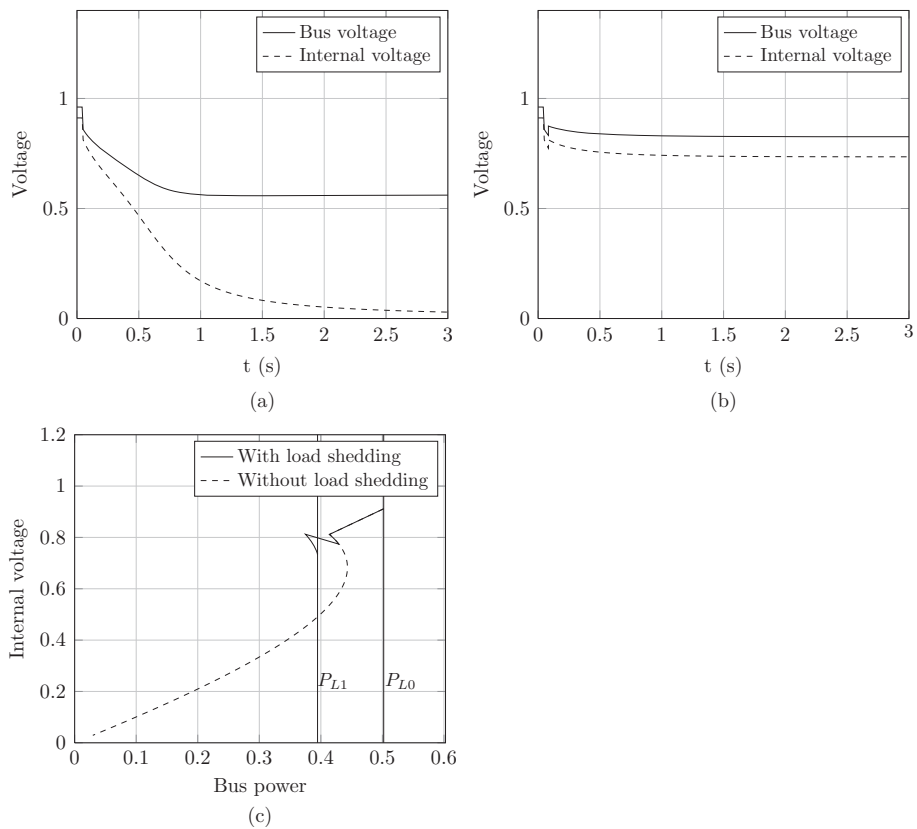


Figure 9: Bus voltage and internal voltage of bus 90 of 162-bus system (a) without load shedding (b) with load shedding, (c) PV curve.

bus 71, as well as at other buses, on the PV curve of bus 71 is explained in detail with reference to Figure 10(C). Point A corresponds to the initial operating point. Following the large disturbance, the operating point moves along BC, part of a PV curve. At C, voltage instability is predicted at buses 71, 85 and 86 and load is shed at the buses. The instant of instability prediction is same at all the buses. The operating point jumps to D and moves along DE before settling at E, drawing power P_{L1} . The load-shedding at buses 85 and 86 influences the post-shedding PV curve at 71, shifting it to the right.

The results of load shedding for the three systems considered are summarized in Table 3. The amount of load to be shed as per the proposed scheme is compared with the minimum amount of load to be shed in order to maintain voltage stability. The comparison is possible only for cases in which instability is detected at a single load bus; it can be seen that the proposed scheme gives load shedding amounts close to the minimum required values.

6 Discussion

The aim of a load shedding scheme, which is employed as a last resort, is to prevent instability so that slower acting devices can act to restore the voltage. The problem of short term voltage instability arises due to fast acting loads. Following a disturbance, fast acting loads tend to draw constant power, thereby leading to voltage collapse at the load bus. While shedding load, it is desirable that the minimum amount of load be shed in the process. This calls for a fast method to determine the amount of load to be shed.

The most important aspects of a load shedding scheme are detection of instability and amount of load to be shed. This work proposes an improvement over the method of using bus voltage as a criterion to shed fixed amount of load after certain delays. The disadvantages of using voltage alone as a criterion to shed fixed amount of loads is that it is not possible to fix the amount *a priori*. Further, if load-shed is insufficient,

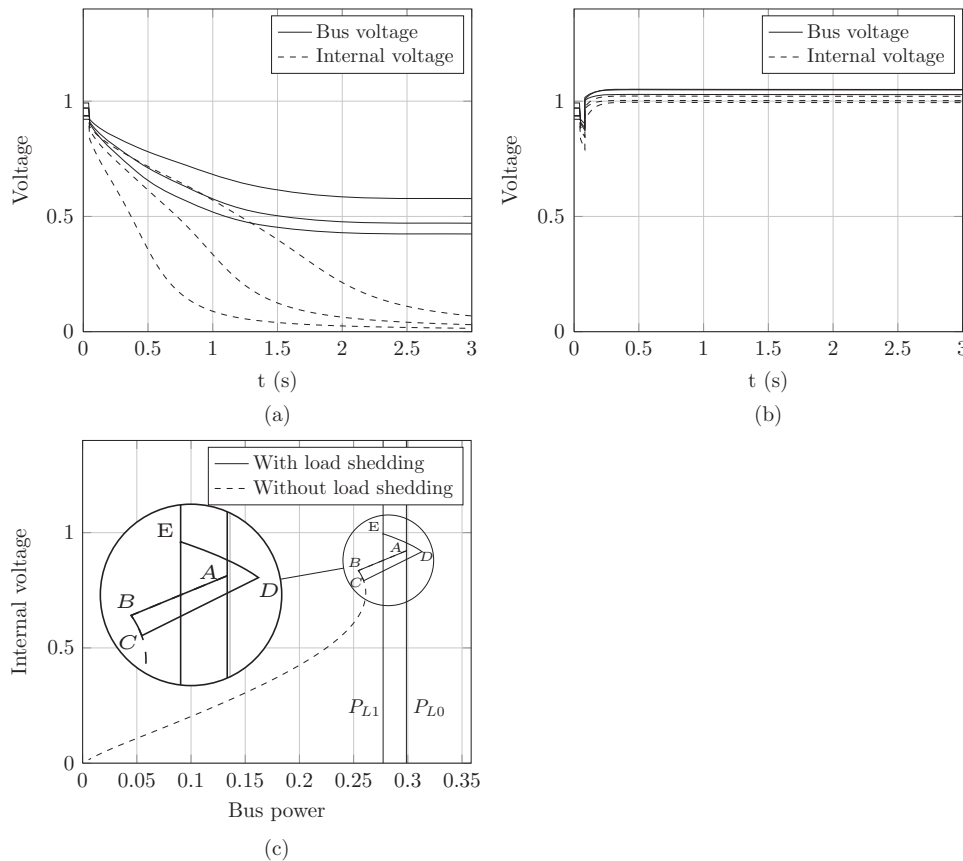


Figure 10: Bus voltage and internal voltage of bus 71, 85, and 86 of 162-bus system when line between buses 71 and 150 is tripped: (a) without load shedding (b) with load shedding, (c) bus 71 PV curves.

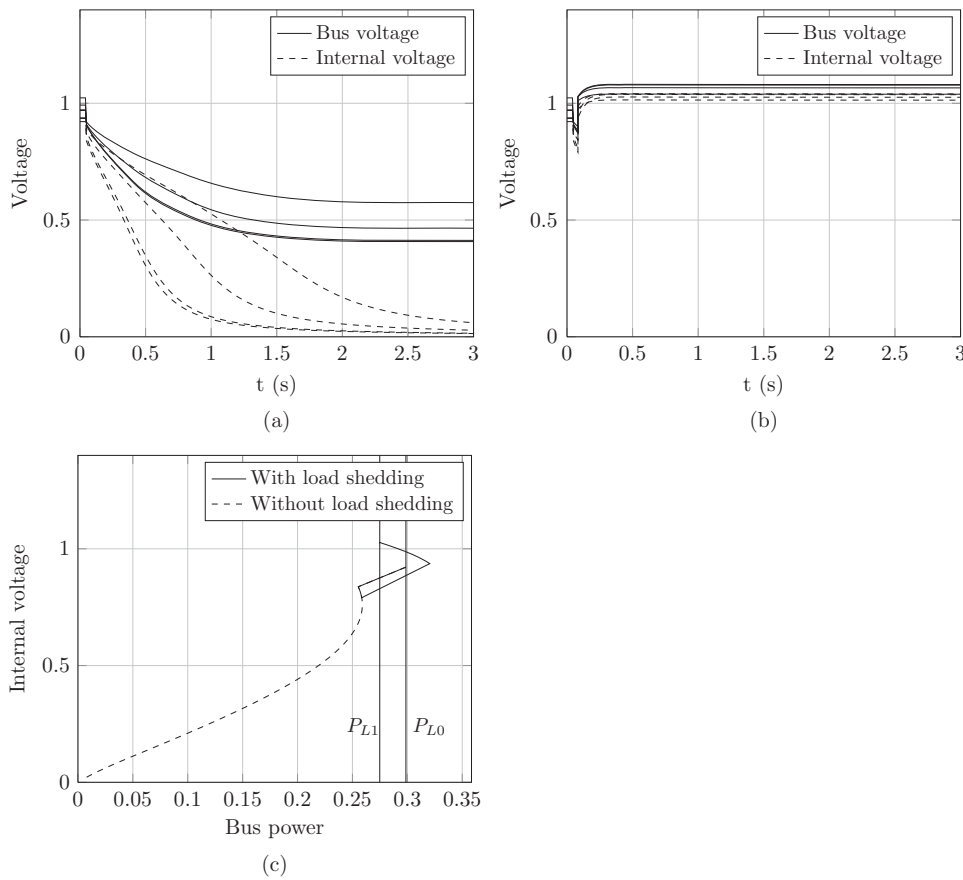


Figure 11: Bus voltage and internal voltage of bus 71, 85, 86, and 150 of 162-bus system when line between buses 149 and 150 is tripped: (a) without load shedding (b) with load shedding, (c) bus 71 PV curves.

Table 3: Comparison of amount of load shed by proposed scheme and minimum required amount.

System	Transmission line tripped	Buses at which voltage collapses	Amount of load to be shed (%)	
			Proposed scheme	Minimum required to maintain stability
9-bus	4–5	5	38.84	31
39-bus	35–36	35	33.24	29
162-bus	89–90	90	20.31	20
162-bus	71–150	71	7.19	–
		85	100.00	–
		86	100.00	–
		71	7.97	–
		85	100.00	–
162-bus	149–150	86	100.00	–
		150	100.00	–
		150	100.00	–

further load-shedding may be necessary. Shedding insufficient load will lead to increased amount of load-shedding to be done at later instants and stability is not assured. This was tried for the 9-bus system. Load-

shedding is carried out for the same disturbance but with voltage alone as a criterion as suggested in Taylor [1]. A fixed amount of load, 5% of remaining load, is shed every time the voltage falls by 5% of the pre-disturbance

value. For comparison with proposed method, voltage measurements are assumed to be taken in the same time interval as the five measurements of bus active power. It was found that this method requires 84% of the load to be shed at bus 5 and 9.75% of the load to be shed at bus 8 in order to restore the voltage to the desired value. On the other hand, the proposed scheme ensures timely shedding of only 38.84% of the load which is slightly higher than the minimum required amount of 31% as shown in Table 3.

Predicting voltage instability helps in minimizing the amount of load shed, unlike as in Vu et al. [4], Balanathan et al. [7], where the criteria for initiating load-shedding is the equivalencing of load and Thevenin impedances. Further, in all cases, while predicting the maximum power P_{\max} using curve fitting, P_{\max} was predicted with sufficient accuracy by the curves fit from the first five measurements. The proposed method relies only on local measurements unlike methods such as Adewole et al. [22] which are centralized schemes that employ wide area measurements. Unlike Deuse et al. [23] in which the amount of load to be shed depends on the initial transformer loading, the proposed method determines the amount of load to be shed based on the prevailing system conditions.

Another important factor taken into account in this work is the change in Thevenin equivalent as seen from the internal bus of the load, post load-shedding. When a large amount of load is shed, it is evident from the model of the load that the Thevenin equivalent, as seen from the internal bus, changes as a consequence of shedding. This factor is taken into account when deciding the amount of load so as to ensure an equilibrium point, post load-shedding. Equations (11), (12) take into account, the change in Thevenin parameters as a consequence of change in the reactance of the load as load is shed. This is done assuming that the network does not contribute to the change in Thevenin parameters after load-shedding. In practice, after load-shedding, the contribution of the network to the change in Thevenin parameters is found to be small.

The proposed method is successful in making the system stable even if, in the course of stability prediction, the nose point of the PV curve is traversed. This allows for inclusion of measurement and circuit-breaker operation delays. Figure 12 shows the PV curves for the 9-bus system for which load-shedding is carried out for the same disturbance but assuming a delay of one cycle of fundamental frequency for measurement and three cycles for circuit-breaker operation; the nose point is already traversed at the instant of load-shedding. The amount of

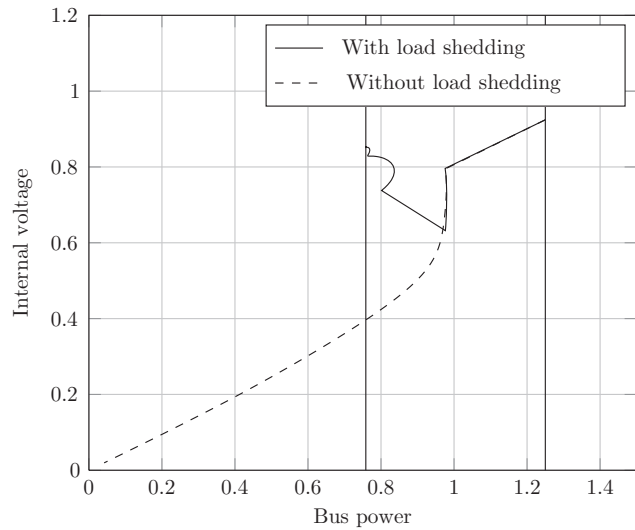


Figure 12: PV curves of 9-bus system with delays for measurement and CB operation accounted for.

load shed is 40%, which is higher than the minimum amount (31%) without assuming any delays. While assuming delays, to ensure stability, a higher required amount may be shed.

The proposed scheme is devised to determine the minimum amount of load required to be shed, and shedding this amount of load results in operation at the nose point with zero margin. In this case, there is a risk of instability arising due to uncertainties in the model and parameter values. Therefore, a margin has to be maintained by shedding the load, the amount of which is slightly higher than the minimum required. However, this requires the knowledge of the minimum amount of load to be shed which is determined by the proposed method. Incidentally, in the cases reported in the paper, the amount of load shed by the proposed method is marginally higher than the minimum required amount.

In this paper, the Thevenin equivalent circuit parameters E_{Th} , R_{Th} , and X_{Th} are defined by (10). It is to be noted that, even during a transient, if the voltages and currents are assumed to be slowly varying phasors, the system can be represented by an equivalent circuit under the following conditions:

1. Generators are represented by certain models such as classical model or two axis model with direct axis and quadrature axis reactances being equal.
2. Load has an equivalent circuit.

The generator equivalent circuit is a variable voltage source in series with a fixed impedance. The load is a variable impedance; for example, in this paper, the load

has an equivalent circuit shown in Figure 1 where conductance G_m is a variable. This results in the Thevenin circuit parameters being not constant and hence estimation of their values is challenging. There are high frequency network transients as well as variations corresponding to a larger time constant (or low frequency oscillations) in the measurements, due to the disturbance. In this work, we have assumed that the high frequency transients would have decayed by the instant of the first measurement. For the systems studied and the disturbances considered, the low frequency oscillations are not significant.

From Table 2, it can be seen that in most of the cases the Thevenin parameters estimated from local measurements are close to the actual values. The Thevenin parameters may be obtained using PMU data as discussed in Abdelkader and Morrow [17]. It can be seen that the method presented in this paper i. e. using (10), is equivalent to the methods described in [4] and [16]. The method in [16] is a reformulation of method in [4]; the method serves to synchronize the three measurements to the same reference by triangulating them.

The results presented in Table 3 show that the proposed method gives fairly accurate results. A comparison of the minimum amount of load to be shed and that given by the method shows that the method gives results close to the minimum amount of load to be shed. Load shed is slightly higher than the minimum amount. This ensures stability. Further, in all cases, a single load-shedding was sufficient and the need for further shedding did not arise. The method is thus simple, fast and efficient in addressing short-term voltage stability.

7 Conclusions

A simple and computationally efficient undervoltage load shedding scheme for avoiding short-term voltage instability is proposed. A method to predict voltage instability by estimating the maximum power on the post-disturbance PV curve using measurements of bus power is suggested. If instability is predicted, an estimate of the amount of load to be shed is obtained using the Thevenin equivalent of the network as seen from the load bus. Thevenin parameters determined from three measurements were found to be comparable with the actual Thevenin parameters. Simulations are carried out on three test systems to validate the scheme. In cases where instability is predicted at a single bus, a comparison with the actual

amount of load to be shed shows that the method gives results close to the actual amount. The method is also successful in preventing instability when voltage collapse is predicted at several buses.

Appendix

8.1 Turbine data

Data for single reheat turbine Kundur [24]:
 $F_{HP} = 0.3$, $T_{RH} = 7.0$ s, Speed droop $R = 5\%$.

References

1. Taylor C. Concepts of undervoltage load shedding for voltage stability. *IEEE Trans Power Del* 1992;7:480–8.
2. Tuan T, Fandino J, Hadjsaid N, Sabonnadiere J, Vu H. Emergency load shedding to avoid risks of voltage instability using indicators. *IEEE Trans Power Syst* 1994;9:341–51.
3. Arnborg S, Andersson G, Hill D, Hiskens I. On undervoltage load shedding in power systems. *Int J Electric Power Energy Syst* 1997;19:141–9.
4. Vu K, Begovic M, Novosel D, Saha M. Use of local measurements to estimate voltage-stability margin. In *Power Industry Computer Applications, 1997. 20th International Conference on*, 1997:318–23.
5. Xu W, Mansour Y. Voltage stability analysis using generic dynamic load models. *IEEE Trans Power Syst* 1994;9:479–93.
6. Balanathan R, Pahalawaththa N, Annakkage U, Sharp P. Undervoltage load shedding to avoid voltage instability. *IEE Proc Gener Transm Distrib* 1998b;145:175–81.
7. Balanathan R, Pahalawaththa N, Annakkage U. A strategy for undervoltage load shedding in power systems. In *Power System Technology, 1998. Proceedings. POWERCON'98. 1998 International Conference on*, volume 2, 1998a:1494–8.
8. Wiszniewski A. New criteria of voltage stability margin for the purpose of load shedding. *IEEE Trans Power Delivery* 2007;22:1367–71.
9. Henriques, R.M, Martins N., Ferraz, J., Martins, A.C, Pinto, H., Sandoval Carneiro Jr. Impact of induction motor loads into voltage stability margins of large systems. In *14th Power Systems Computing Conference, 2002, Sevilha, 2002*.
10. Abe S, Fukunaga Y, Isono A, Kondo B. Power system voltage stability. *IEEE Trans Power App Syst* 1982;PAS-101:3830–40.
11. Sekine Y, Ohtsuki H. Cascaded voltage collapse. *IEEE Trans Power Syst* 1990;5:250–6.
12. Ohtsuki H, Yokoyama A, Sekine Y. Reverse action of on-load tap changer in association with voltage collapse. *IEEE Power Eng Rev* 1991;11:300–6.
13. Pal M. Voltage stability conditions considering load characteristics. *IEEE Trans Power Syst* 1992;7:243–9.

14. Pal M. Voltage stability: analysis needs, modelling requirement, and modelling adequacy. *IEE Proc Gener Transm Distrib* 1993;140:279–86.
15. IEEE. Standard load models for power flow and dynamic performance simulation. *IEEE Trans Power Syst* 1995;10:1302–13.
16. Corsi S, Taranto G. A real-time voltage instability identification algorithm based on local phasor measurements. *IEEE Trans Power Syst* 2008;23:1271–9.
17. Abdelkader S, Morrow D. Online tracking of Thevenin equivalent parameters using PMU measurements. *IEEE Trans Power Syst* 2012;27:975–83.
18. Octave GNU. GNU Octave 3.2.4. Available at: <http://www.octave.org>.
19. Sauer P, Pai M. *Power system dynamics and stability*. Delhi: Prentice Hall, 1998.
20. Padiyar K. *Power system dynamics*. Hyderabad: BS Publications, 2002.
21. Power System Test Case Archive. University of Washington Power System Test Case Archive. Available at: <http://www.ee.washington.edu/research/pstca/>.
22. Adewole AC, Tzoneva R, Apostolov A. Adaptive under-voltage load shedding scheme for large interconnected smart grids based on wide area synchrophasor measurements. *IET Gener Transm Distrib* 2016;10:1957–68.
23. Deuse J, Dubois J, Fanna R, Hamza I. EWR under voltage load shedding scheme. *IEEE Trans Power Syst* 1997;12:1446–54.
24. Kundur P. *Power system stability and control*. EPRI power system engineering series. Delhi: McGraw-Hill Education (India) Pvt Limited, 1994.